Structure and reactivity relationships in *trans*-[PtPh(L)₂Cl] as observed from Cl⁻ anation by I⁻ upon interchanging phosphine, arsine and stibine (L) ligands†

Authors:
Stefanus Otto#*,
Orbett T. Alexander and
Andreas Roodt*

Affiliations:
Department of Chemistry, University of the Free State, P.O. Box 339, Bloemfontein, 9300, South Africa

Corresponding authors:
Stefanus Otto
Fanie.Otto@Sasol.com
Fax: +27-11-5223218
Andreas Roodt
Roodta@ufs.ac.za
Fax:+27-51-4446384

Square-planar chloride for iodide substitution reactions *trans* to a phenyl σ-C was kinetically investigated in a series of sterically congested platinum(II) complexes of the form *trans*-[PtPh(L)₂Cl] (L = PPh₃, **1**; PPh₂Fc, **2**; AsPh₃, **3**; SbPh₃, **4**) in chloroform solution. The reactions follow the normal associative mode of activation, but with equilibria present in all steps. The rate constants for the direct pathway, k_{12}, are $(0.37 \pm 0.03) \times 10^{-3}$ and 0 M⁻¹ s⁻¹ for **1** and **2** at 40 °C, and $(1.6 \pm 0.3) \times 10^{-3}$ and $(143 \pm 10) \times 10^{-3}$ M⁻¹ s⁻¹ for **3** and **4** at 25 °C. The corresponding rate constants for the solvent assisted pathway, k_{13}, are $(0.66 \pm 0.03) \times 10^{-4}$ and $(2.0 \pm 0.2) \times 10^{-4}$ s⁻¹ for **1** and **2** at 40 °C and $(4.1 \pm 0.6) \times 10^{-4}$ and $(1105 \pm 14) \times 10^{-4}$ s⁻¹ for **3** and **4** at 25 °C. The activation parameters for **3** and **4** were determined as $\Delta H^{\neq} = 99.8 \pm 0.6$ and 31 ± 1 kJ mol⁻¹ and $\Delta S^{\neq} = 36 \pm 2$ and -157 ± 4 J K⁻¹ mol⁻¹ for the direct route, k_{12}, and $\Delta H^{\neq} = 45 \pm 2$ and 22.91 ± 0.11 kJ mol⁻¹ and $\Delta S^{\neq} = -181 \pm 7$ and -207.3 ± 0.4 J mol⁻¹ K⁻¹ for the solvent assisted, k_{13}, pathways respectively. The crystal structures of *trans*-[PtPh(PPh₂Fc)₂Cl], *trans*-[PtPh(AsPh₃)₂Cl], *trans*-[PtPh(SbPh₃)₂Cl] and *trans*-[PtPh(SbPh₃)₂I] are reported. Structure and reactivity relationships (of almost *four orders-of-magnitude*) are presented based on kinetic data, multi-nuclear NMR measurements and the crystallographic data.

Waargenome struktuur- en reaktiwiteitsverwantskappe in *trans*-[PtPh(L)₂Cl] tydens die verplasingreaksie van Cl⁻ deur I⁻ na verandering van die fosfien-, arsien- en stibienligande (L): Vierkantig-planêre chloried vir jodied stubstitusiereaksies *trans* ten opsigte van 'n feniel σ-C binding is kineties ondersoek in chloroform vir 'n reeks steries-gestremde platinum(II) komplekse van die vorm *trans*-[PtPh(L)₂Cl] (L = PPh₃, **1**; PPh₂Fc, **2**; AsPh₃, **3**; SbPh₃, **4**). Die reaksies volg die normale assosiative aktivering, maar met ewewigte teenwoordig in alle stappe. Die tempokonstantes vir die direkte roete k_{12}, is onderskeidelik $(0.37 \pm 0.03) \times 10^{-3}$ en 0 M⁻¹ s⁻¹ vir **1** en **2** by 40°C, en $(1.6 \pm 0.3) \times 10^{-3}$ en $(143 \pm 10) \times 10^{-3}$ M⁻¹ s⁻¹ vir **3** en **4** by 25°C. Die ooreenstemmende tempokonstantes vir die oplosmiddelroete, k_{13}, is onderskeidelik $(0.66 \pm 0.03) \times 10^{-4}$ en $(2.0 \pm 0.2) \times 10^{-4}$ s⁻¹ vir **1** en **2** by 40°C en $(4.1 \pm 0.6) \times 10^{-4}$ en $(1105 \pm 14) \times 10^{-4}$ s⁻¹ vir **3** en **4** by 25°C. Die aktiveringsparameters vir **3** en **4** is bepaal as $\Delta H^{\neq} = 99.8 \pm 0.6$ en 31 ± 1 kJ mol⁻¹, met $\Delta S^{\neq} = 36 \pm 2$ en -157 ± 4 J K⁻¹ mol⁻¹ vir die direkte roete, k_{12}, en $\Delta H^{\neq} = 45 \pm 2$ en 22.91 ± 0.11 kJ mol⁻¹ en $\Delta S^{\neq} = -181 \pm 7$ en -207.3 ± 0.4 J mol⁻¹ K⁻¹ vir die oplosmiddelroete, k_{13} onderskeidelik. Die kristalstrukture van *trans*-[PtPh(PPh₂Fc)₂Cl], *trans*-[PtPh(AsPh₃)₂Cl], *trans*-[PtPh(SbPh₃)₂Cl] en *trans*-[PtPh(SbPh₃)₂I] word gerapporteer. Struktuur- en reaktiwiteitsverwantskappe (van ongeveer vier ordegroottes) word bespreek, gebaseer op kinetiese data, multikern KMR-metings en die kristallografiese data.

Introduction

Substitution reactions are very important in many fundamental and applied processes such as catalytic conversions, metal extraction, medicinal inorganic chemistry and environmental reactions, typically associated with carbon dioxide fixation (Johnstone, Suntharalingam and Lippard 2016) (Dobrynin, et al. 2019) (Warsink, et al. 2018). In this regard, square-planar metal complexes provide many examples of model homogeneous catalysts in a range of industrial

----

† Electronic supplementary information (ESI) available: Observed pseudo-first order rate constants for all reactions investigated. Full crystallographic details for *trans*-[PtPh(PPh₂Fc)₂Cl], *trans*-[PtPh(AsPh₃)₂Cl], *trans*-[PtPh(SbPh₃)₂Cl] and *trans*-[PtPh(SbPh₃)₂I] have been deposited with the Cambridge Crystallographic Data Centre, with codes CCDC 1924084, CCDC 1923815, CCDC 1923846 and CCDC 1923876, respectively.

\# Currently employed at: Sasol Technology Research & Development, 1 Klasie Havenga Road, Sasolburg, 1947, South Africa

processes. These substitution reactions usually follow an associative mode of activation almost without exception; however, some examples of a dissociative activation have been confirmed. (Lanza, Minniti, et al. 1984a) (Lanza, Minnitti, et al. 1984b) (Wendt, Deeth and Elding 2000) The reaction rates are dependent on a range of factors such as the nature of the *cis* and *trans* ligands, the charges of the reacting species, the solvent, the leaving group, as well as the nature and concentration of the entering nucleophile. Steric and electronic factors may favour/disfavour the addition of a fifth ligand to form a five-coordinate 18-electron transition state in contrast to the loss of a ligand resulting in a 14-electron, three-coordinate intermediate. More recent examples of literature studies which include kinetic evaluations are referenced below. (Hoffmann, et al. 2015) (Johnstone, Suntharalingam and Lippard 2016) (Crespo, et al. 2014) (Bugarčić, et al. 2012).

Two parallel pathways are normally encountered for square-planar substitution reactions which involve the direct attack of the entering nucleophile on the complex to form the product, or via a solvent assisted reactive intermediate. In particular, when equilibria are present in the reaction for all the separate steps as highlighted in Scheme 1, more complex behaviour of the pseudo first-order rate constant (Eqn. 1; [Cl⁻], [I⁻] >> [Pt]) is encountered. (Seguin and Zador 1976) (De Waal and Robb 1978) (Elding and Gröning 1980) (Otto, Botha and Roodt 2018).
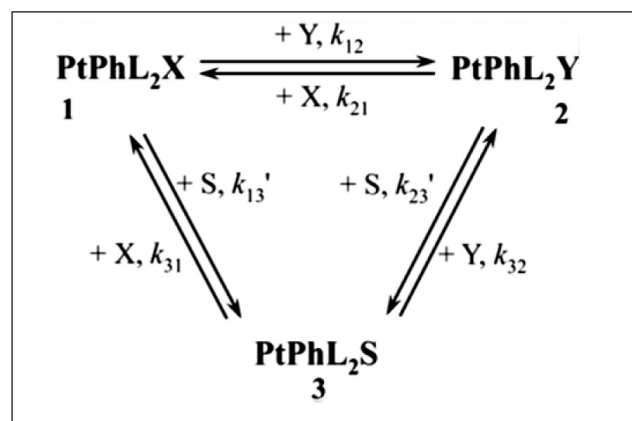
SCHEME 1: Schematic presentation of a square-planar substitution reaction of X (Cl⁻) by Y (I⁻) in the phenyl complex *trans*-[PtPh(L)₂X] as described in this study, showing the parallel direct substitution- and solvent-assisted pathways, where [PtPhL₂X]= [PtPhL₂Cl] = 1, [PtPhL₂Y] = [PtPhL₂I] = 2 and [PtPhL₂S] = 3. The subscripts of the rate constants denote the numbers of the species involved in the specific reaction, e.g. k_{12} indicates the rate constant for the reaction proceeding from complex 1 to 2. The solvent (S) concentration is incorporated in the rate constants k_{13} and k_{23}, where $k_{13} = k_{13}'$[S] and $k_{23} = k_{23}'$[S], respectively. ([S] denotes the concentration of the solvent; 12.50 mol dm⁻³ for CHCl₃ at 25 °C).

$$k_{obs} = k_{12}\left([Y] + \frac{[X]}{K_{eq}}\right) + \frac{\frac{k_{13}}{K_{eq}}\frac{k_{32}}{k_{31}}[X] + k_{13}\frac{k_{32}}{k_{31}}[Y]}{[X] + \frac{k_{32}}{k_{31}}[Y]} \quad (1)$$

In Eq. 1, K_{eq} denotes the equilibrium constant for the formation of complex 2 and is defined as the rate of the forward reactions divided by the rate of the reverse reactions (Eq. 2), with equilibria present in the direct- and solvent-assisted pathways.

$$K_{eq} = \frac{k_{12}}{k_{21}} = \frac{k_{13}k_{32}}{k_{23}k_{31}} \quad (2)$$

If the equilibrium favours the formation of complex 2 ($K_{eq} \gg 1$), Eq. 2 simplifies to the well-known two-term rate law (Eq. 3) for square-planar substitution reactions.

$$k_{obs} = k_{12}[Y] + k_{13} \quad (3)$$

A large number of examples of square-planar substitution reactions have been discussed in a previous paper, and the reader is referred to those for further background (Baddley and Basolo 1966) (Goddard and Basolo 1968) (Palmer and Kelm 1975) (Roulet and Gray 1972) (Van Eldik, et al. 1981) (Palmer, et al. 1978) (Van Eldik, et al. 1981) (Pienaar, Kotowski and Van Eldik 1989) (Berger, et al. 1989) (Elding, Kellenberger and Venanzi 1983) (Cusumano, et al. 1979) (Ricevuto, Romeo and Trozzi 1974) (Minnitti, et al. 1987) (Frey, et al. 1989) (Romeo, Grassi and Scolaro 1992). Other reactions involving square-planar complexes that proceed through three coordinated transition states include the uncatalysed *cis* to *trans* isomerisation of complexes of the type *cis*-[PtR(PEt₃)₂X] (R = alkyl or aryl; X = solvent molecule or halide ion) (Alibrandi, Scolaro and Romeo 1991) (Alibrandi, Cusumano, et al. 1989) (Romeo, Alibrandi and Scolaro 1993) (Kubota, et al. 1982) (Scott and Puddephatt 1983).

For more recent examples of detailed kinetic studies on these types of systems the reader is referred to a number of example literature reports (Hoffmann, et al. 2015) (Johnstone, Suntharalingam and Lippard 2016) (Maidich, et al. 2013) (Otto, Botha and Roodt 2018) (Crespo, et al. 2014) (Bugarčić, et al. 2012) (Hennion, et al. 2013).

In spite of the fact that complexes with platinum(IV)-carbon σ-bonds were first reported over 100 years ago (Pope and Peachey 1907) it was not until the late 1950's that the first complexes containing platinum(II)-carbon σ-bonds were prepared, (Chatt, Vallarino and Venanzi 1957) and specifically those containing platinum(II)-methyl σ-bonds were described (Chatt and Shaw 1959).

A previous report (Otto and Roodt 2006) illustrated the kinetic behaviour of *trans*-[Pt**Me**(SMe₂)₂Cl] towards anionic and neutral ligands with different entering monodentate nucleophiles. Moreover, in a recent paper (Otto, Botha and Roodt 2018) detailed results were also presented of the chloride anation by iodide, in chloroform solution, *trans* to a strong labilising group (Me⁻ and H⁻) in systems containing ligands with group 15 donor atoms. The reactions followed the normal associative mode of activation, but with equilibria present in all steps. Structure and reactivity relationships were presented based on kinetic data, multi-nuclear NMR measurements and the crystallographic data. These emphasised the dependence of the pseudo first-order

rate constant on the electro-steric effects of the combination of *cis* and strong sigma-donating *trans* ligand. A more than four orders-of-magnitude reactivity range was observed.

In this current paper the focus is expanded to chloride substitution by iodide *trans* to a bulky **phenyl** σ-C group, thus significantly increasing the steric bulk around the Pt(II), but at the same time as an aryl moiety offering also an electronic variation compared a simple alkyl group such as methyl. Thus, a detailed kinetic study on complexes of the form *trans*-[PtPh(L)$_2$Cl] (L = PPh$_3$, PPh$_2$Fc, AsPh$_3$ and SbPh$_3$), where the *cis* ligands were expanded down Group 15 donor atoms to also include SbPh$_3$. This relates to other literature studies (Otto and Roodt 2002a) (Otto and Roodt 2002b) (Otto and Roodt 2008) on the coordination behaviour of the SbPh$_3$ ligand in rhodium systems in the solid- and solution state and now extends the investigation to also include platinum based complexes. Specifically, for the stibine ligands, not much kinetic data is available, as had been highlighted fairly recently (Hennion, et al. 2013).

Materials and Methods

General

All chemicals used for the preparation of the complexes were of reagent grade. The following metal complexes and ligands were available commercially: K$_2$PtCl$_4$ (Next Chimica); SMe$_2$ (Merck); NaBPh$_4$ (Aldrich); PPh$_3$ (Merck); AsPh$_3$ (Merck) and SbPh$_3$ (Merck). All other reagents and solvents were of the best quality available.

The complexes were identified using ^{1}H, ^{13}C, ^{31}P and ^{195}Pt NMR (Bruker operating at 300, 75.468, 121.497 and 64.525 MHz respectively). All NMR spectra were recorded in CDCl$_3$, the ^{1}H spectra were calibrated relative to the residual CHCl$_3$ peak (7.24 ppm) and the ^{13}C NMR spectra were calibrated relative to the chloroform ^{13}C resonance (77.66 ppm). From the ^{13}C NMR spectra only the chemical shift, together with the first order Pt-C coupling constant, of the carbon directly attached to the platinum is reported. The ^{31}P NMR spectra were calibrated relative to 85% H$_3$PO$_4$ as an internal standard in a capillary (0 ppm) and the ^{195}Pt NMR spectra relative to K$_2$PtCl$_4$ as external standard (-1639 ppm).

Preparation of complexes

The mixture of *cis*- and *trans*-[PtCl$_2$(SMe$_2$)$_2$] and PPh$_2$Fc was prepared according to the procedures of Otto (Otto and Roodt 2006) and Sollot (Sollot, et al. 1963) respectively. The solution behaviour of the respective complexes towards iodide was investigated *in situ* by appropriate NMR measurements.

trans-**[PtPh(SMe$_2$)$_2$Cl].** A mixture of *cis*- and *trans*-[PtCl$_2$(SMe$_2$)$_2$] (500 mg; 1.3 mmol) was dissolved in dichloromethane (10 mL) and NaBPh$_4$ (445 mg; 1.3 mmol) was added. The resulting suspension was stirred for a week and filtered to remove the NaCl formed during the reaction.

Purification on a silica column (hexane/ acetone; 8/ 2) yielded the pure product (387 mg; 70%). ^{1}H NMR: δ 2.31 (t, 12H, $^3J_{Pt-H}$ = 58 Hz); 6.9 - 7.0 (m, 3H); 7.3 (m, 2H).

trans-**[PtPh(PPh$_3$)$_2$Cl], Ia.** *trans*-[PtPh(SMe$_2$)$_2$Cl] (100 mg; 0.23 mmol) was dissolved in acetone (10 mL) and PPh$_3$ (184 mg; 0.70 mmol), also dissolved in acetone (5 mL), was added without stirring. Slow evaporation of the acetone yielded the crystalline product, which was washed with ether to remove traces of unreacted phosphine. The use of more concentrated solutions or a larger excess of phosphine leads to rapid precipitation of the product in approximate quantitative yields (189 mg; 98%). ^{1}H NMR: δ 6.09 (t, 2H); 6.25 (t, 1H); 6.62 (td, 2H); 7.18 - 7.34 (m, 18H); 7.45 - 7.55 (m, 12H). ^{31}P NMR: δ 24.95 (t, $^1J_{Pt-P}$ = 3151 Hz). ^{195}Pt NMR: δ -4377 (t, $^1J_{Pt-P}$ = 3142 Hz). Anal. Calc. for C$_{42}$ H$_{35}$ Cl P$_2$ Pt (832.206): C, 60.62; H, 4.24. Found C, 60.81; H, 4.41.

trans-**[PtPh(PPh$_3$)$_2$I], Ib.** The complex *trans*-[PtPh(PPh$_3$)$_2$Cl] (10 mg; 0.012 mmol) was dissolved in CDCl$_3$ (3 mL) in an NMR tube (10 mm) and Bu$_4$NI (44 mg; 0.12 mmol) was added, the reaction progress as followed by ^{31}P NMR indicated smooth conversion of the parent chlorido complex to the corresponding iodido complex. ^{31}P NMR: δ 24.21 (t, $^1J_{Pt-P}$ = 3134 Hz).

trans-**[PtPh(PPh$_2$Fc)$_2$Cl], IIa**. The same general procedure was used as described for **Ia**. Recrystallisation from benzene yielded crystals suitable for X-ray analysis (237 mg; 98%). ^{1}H NMR: δ 3.81 (m, 4H); 4.22 (m, 4H); 4.31 (s, 10H); 6.35 (t, 2H); 6.49 (t, 1H); 6.82 (td, 2H); 7.21 - 7.34 (m, 12H); 7.42 - 7.52 (m, 8H). ^{31}P NMR: δ 16.34 (t, $^1J_{Pt-P}$ = 3142 Hz). ^{195}Pt NMR: δ -4300 (t, $^1J_{Pt-P}$ = 3136 Hz). Anal. Calc. for C$_{50}$ H$_{43}$ Cl P$_2$ Fe$_2$ Pt (1048.045): C, 57.30; H, 4.14. Found C, 57.52; H, 4.31.

trans-**[PtPh(PPh$_2$Fc)$_2$I], IIb**. The same general procedure was used as described for **Ib**. ^{31}P NMR: δ 13.17 (t, $^1J_{Pt-P}$ = 3066 Hz).

trans-**[PtPh(AsPh$_3$)$_2$Cl], IIIa**. The same general procedure was used as described for **Ia**. Utilisation of more diluted acetone solutions of *trans*-[PtPh(SMe$_2$)$_2$Cl] and AsPh$_3$ yielded crystals suitable for X-ray analysis (209 mg; 97%). ^{1}H NMR: δ 6.18 (t, 2H); 6.29 (t, 1H); 6.75 (td, 2H); 7.20 - 7.35 (m, 18H); 7.42 - 7.48 (m, 12H). ^{13}C NMR: δ 131.45 (t, $^1J_{Pt-C}$ = 830 Hz). ^{195}Pt NMR: δ -4316 (s). Anal. Calc. for C$_{42}$ H$_{35}$ Cl As$_2$ Pt (920.101): C, 54.83; H, 3.83. Found C, 54.62; H, 3.98.

trans-**[PtPh(AsPh$_3$)$_2$I], IIIb**. The same general procedure was used as described for **Ib** with the exception that ^{195}Pt NMR was used to verify conversion to the desired product. ^{195}Pt NMR: δ -4738 (s).

trans-**[PtPh(SbPh$_3$)$_2$Cl], IVa**. The same general procedure was used as described for **Ia**. Utilisation of a more dilute acetone solution of *trans*-[PtPh(SMe$_2$)$_2$Cl] and SbPh$_3$ yielded yellow plates suitable for X-ray analysis (153 mg; 65%). ^{1}H

NMR: δ 6.44 (m, 3H); 7.10 (m, 2H); 7.25 - 7.38 (m, 18H); 7.39 - 7.44 (m, 12H). ^{195}Pt NMR: δ -4136 (s). Anal. Calc. for $C_{42}H_{35}$ Cl Sb_2 Pt (1013.778): C, 49.76; H, 3.48. Found C, 50.07; H, 3.72.

***trans*-[PtPh(SbPh$_3$)$_2$I], IVb**. The same general procedure was used as described for **IIIb**, in addition crystals suitable for X-ray diffraction were obtained upon slow evaporation of the NMR sample. ^{195}Pt NMR: δ -4689 (s). Anal. Calc. for $C_{42}H_{35}$ I Sb_2 Pt (1105.230): C, 45.64; H, 3.19. Found C, 46.43; H, 3.61.

Kinetics measurements

Note that the liquid state reactants studied kinetically are denoted by *Arabic numericals* **1 – 4**, also when referred to literature complexes, **5 – 10**, as discussed below. UV-Vis and time resolved spectra for the slower reactions were recorded on a Cary 300 Bio spectrophotometer equipped with a temperature regulator. Time resolved data for the faster reactions were collected with a Durram D110 stopped-flow system equipped with a temperature regulating unit. In all cases, except for **2**, the reactions were carried out in dried and distilled chloroform with a final metal concentration of 0.25 mmol dm^{-3}. In the UV

investigation of **2**, kinetic traces with limited reproducibility (large esd's) were observed, assumed to be linked to (i) the significant contribution of the ferrocene fragment to the nett absorbance, and (ii) coupled with the small equilibrium constant. The values for k_{obs} were subsequently determined using ^{31}P NMR with [Pt] = 2.5 mmol dm^{-3}. All reactions contained additional added chloride amounting to a final concentration of 2.5 mM, except those for **1** and **2** which contained no additional chloride. The final iodide concentrations were varied in the range 2.5 – 150 mM while maintaining a ten-fold excess of iodide to metal to ensure pseudo first order reaction conditions in all cases. Complexes **1** and **2**, were only investigated at 40 °C due to their low reactivity while complexes **3** and **4** were investigated at 10, 25 and 40 °C in order to obtain activation parameters for these systems. The observed rate constants were obtained from the absorbance *vs.* time traces using the least-squares programmes SCIENTIST (MicroMath 1990) for the UV data and OLIS (On-Line Instrument-Systems Inc.) for the stopped-flow data. Rate constants determined by stopped-flow techniques are given as the average of at least five individual runs. The observed pseudo first order rate constants were fitted versus the ligand concentrations using the extended rate expression for square-planar

TABLE 1: Crystallographic data and refinement parameters for **IIa**, **IIIa**, **IVa** and **IVb**.

	IIa	IIIa	IVa	IVb
Emp. formula	$C_{50}H_{43}ClFe_2P_2Pt$	$C_{42}H_{35}As_2ClPt$	$C_{42}H_{35}ClSb_2Pt$	$C_{42}H_{35}ISb_2Pt$
Form. weight	1048.02	920.08	1013.74	1105.19
Crystal system	Monoclinic	Orthorhombic	Monoclinic	Triclinic
Space group	$C2/c$	$Pbca$	$C2/c$	$P\bar{1}$
a/ Å	13.581(3)	33.595(2)	16.508(3)	11.3655(3)
b/ Å	17.865(4)	19.7316(13)	11.1760(10)	12.9484(4)
c/ Å	17.593(4)	10.7505(7)	19.989(3)	13.6154(4)
α/ °	90	90	90	80.178(1)
β/ °	105.91(3)	90	95.660(10)	70.443(1)
γ/ °	90	90	90	79.059(1)
V/ Å^3	4105.1(14)	7126.4(8)	3669.9(9)	1841.34(9)
Z	4	8	4	2
D_c/ g.cm^{-3}	1.696	1.715	1.835	1.933
μ/ mm^{-1}	4.276	5.885	5.365	6.122
Tmax/ Tmin	0.536/ 0.258	0.536/ 0.258	0.199/ 0.037	0.675/ 0.234
F(000)	2080	3584	1936	1040
Crystal size/ mm	0.30x0.20x0.16	0.40x0.30x0.28	0.30x0.22x0.12	0.35x0.24x0.15
θ limit/ °	2.04 to 30.51	2.06 to 26.02	2.20 to 29.57	2.08 to 29.57
Index ranges	-19 ≤ h ≤ 19	-41 ≤ h ≤ 35	-21 ≤ h ≤ 22	-15 ≤ h ≤ 15
	-24 ≤ k ≤ 25	-24 ≤ k ≤ 24	-15 ≤ k ≤ 15	-12 ≤ k ≤ 17
	-25 ≤ l ≤ 24	-13 ≤ l ≤ 12	-27 ≤ l ≤ 26	-18 ≤ l ≤ 18
Collected refl.	20616	39925	17714	18204
Unique refl.	6205	7014	5140	10233
R_{int}	0.0395	0.0668	0.0516	0.0565
Obs. refl. ($I>2(\sigma)I$)	4843	5036	3821	8118
Data/ rest./ param.	6205/ 0/ 255	7014/ 0/ 415	5140/ 0/ 210	10233/ 0/ 416
GooF	0.968	1.097	1.040	0.979
R ($I>2(\sigma)I$) R^a	0.0283	0.0484	0.0389	0.0344
wR^b	0.0568	0.1025	0.0944	0.0787
R (all data) R	0.0463	0.0809	0.0608	0.0503
wR	0.0606	0.1159	0.1065	0.0839
$\Delta\rho_{max}$; $\Delta\rho_{min}$/ e.Å^{-3}	0.624; -0.992	2.493; -1.282	0.912; -1.769	1.942; -1.582

a) $R = [(\Sigma\Delta F)/(\Sigma F_o)]$ b) $wR = \Sigma[w(F_o^2 - F_c^2)^2]/\Sigma[w(F_o^2)^2]^{1/2}$

substitution given in Eqn. 1, while the activation parameters were calculated from the exponential form of the Eyring equation (Plutino, et al. 1999).

Crystallography

Note that the solid-state products and structures analysed are denoted by *Roman numericals* **I – IV**. Crystals suitable for X-ray diffraction were obtained as described in the experimental section. All X-ray diffraction intensity data were collected as ω-scans at 293(2) K on a Siemens SMART CCD diffractometer using Mo K$_\alpha$ (0.71073 Å) from a rotating anode source. Reflections were merged and integrated using SAINT and were corrected for Lorentz, polarisation and absorption effects using SADABS (Bruker-AXS-Inc. 2007). After completion of the data collection the first 50 frames were repeated to check for decay of which none was observed. The structures were solved by the heavy atom method and refined through full-matrix least squares cycles using the SHELXL97 software package (Sheldrick 2008) with $\Sigma(/F_o/-/F_c/)^2$ being minimised. All non-H atoms were refined with anisotropic displacement parameters while the H atoms were constrained to parent sites using a riding model. The graphics were done with DIAMOND (Brandenburg 1998). Crystallographic data, details of the data collection and refinement parameters for **IIa**, **IIIa, IVa** and **IVb** are given in Table 1.

Results and Discussion

Synthesis and NMR characterisation

The complexes were prepared as described in the experimental section and unambiguously characterised by multinuclear NMR spectroscopy and X-ray crystallography. In general, phenyl complexes of Pt(II) containing group 15 donor ligands can be prepared by the substitution of SMe$_2$ or COD from *trans*-[PtPh(SMe$_2$)$_2$Cl] or [PtPh(COD)Cl] or by the action of a phenyl lithium or a Grignard reactant on the appropriate *cis*-[Pt(Cl)$_2$(L)$_2$] complex. The preparation of choice was, however, by utilisation of phenyl transfer from BPh$_4^-$ in the SMe$_2$ complex using a modification of the

procedure developed by (Kukushkin, et al. 1992). This procedure gives a high yield of pure *trans*-[PtPh(SMe$_2$)$_2$Cl] and even though reaction times of a week is required it is not labour intensive and no special precautions against moisture is required. The *trans*-[PtPh(SMe$_2$)$_2$Cl] complex is sufficiently stable to be stored for extended periods of time and the SMe$_2$ ligands could be substituted with relative ease by all ligands used in the current study.

Crystallography

Note that the solid-state products and structures analysed are denoted by *Roman numericals* **I – IV**. In order to fully characterise the complexes used in the kinetic investigation a thorough crystallographic study was performed. Especially the composition of the arsine and stibine complexes, **IIIa** and **IVa**, are difficult to determine unambiguously using other techniques, such as IR spectroscopy and even ^{1}H, ^{13}C or ^{195}Pt NMR spectroscopy. Furthermore, it was anticipated to make correlations between parameters observed in the solid ground state (X-ray crystallography), in the solution ground state (NMR) and in the solution activated state (kinetics) (Roodt, Visser and Brink 2011). Selected geometrical parameters are thus presented in Table 2 while molecular diagrams showing the numbering scheme and thermal ellipsoids are shown in Figures 1 and 2 respectively.

The structures of **IIa**, **IIIa** and **IVa** show that the complexes all exhibit distorted square-planar geometries around the Pt(II) centre with the bulky tertiary phosphine, arsine and stibine ligands in a *trans* orientation with respect to one another. Complexes **IIIa** and **IVa** represent less common examples of structural studies on *bis*-arsine and -stibine complexes of Pt(II), which have not received that much attention in literature (Allen 2002).

It was reported previously (Otto, Roodt and Leipoldt 1995) (Otto, Botha and Roodt 2018) (Roodt, Otto and Steyl 2003) that the related *trans*-[PtMe(L)$_2$Cl] (L = tertiary phosphine ligands) complexes are prone to disorders in the methyl- and chlorido positions (typically through inversion
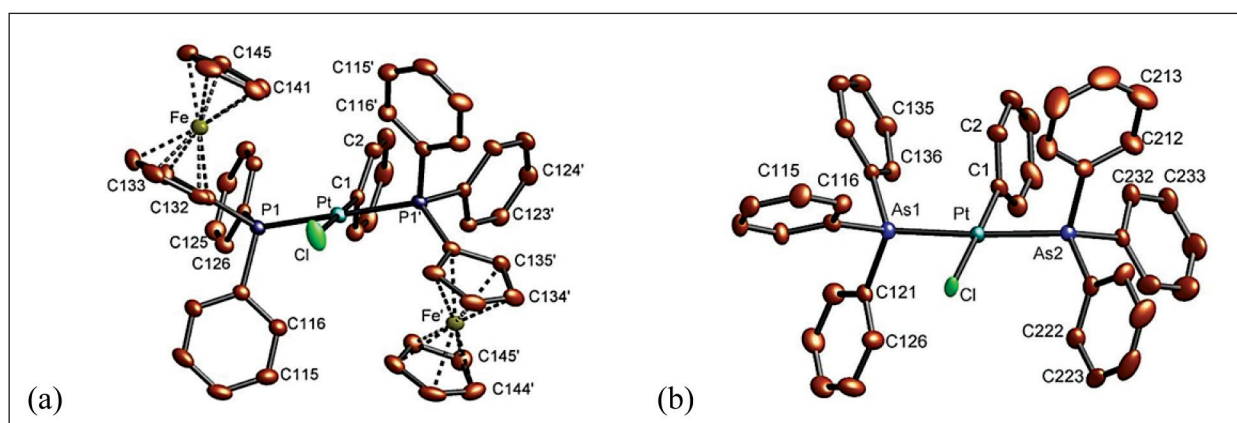
FIGURE 1: Molecular diagram showing the numbering scheme and displacement ellipsoids (30% probability), with hydrogen atoms omitted for clarity for (a) **IIa**, and (b) **IIIa**. In the numbering scheme of the aromatic rings the first digit refers to the number of the ligand, the second to the number of the ring (1 - 4) and the third to the number of the atom in the ring (1 - 6 for Ph and 1 - 5 for Cp).

TABLE 2: Selected geometrical parameters for **IIa**, **IIIa**, **IVa** and **IVb**.

	IIa	IIIa	IVa	IVb
Pt-Cl	2.3988(12)	2.4575(18)	2.387(2)	2.6805(3)*
Pt-C1	2.022(4)	2.042(8)	2.018(6)	2.037(4)
Pt-L1	2.3298(8)	2.3982(8)	2.5419(5)	2.5353(3)
Pt-L2		2.3990(8)		2.5450(3)
L1-C111	1.830(3)	1.945(8)	2.113(5)	2.136(4)
L1-C121	1.827(3)	1.936(8)	2.127(5)	2.142(5)
L1-C131	1.807(3)	1.945(8)	2.121(5)	2.133(4)
L2-C211		1.929(8)		2.136(4)
L2-C221		1.929(8)		2.127(5)
L2-C231		1.955(8)		2.140(4)
L1-L2	4.660(1)	4.794(1)	5.080(1)	5.010(1)
L1-Pt-L2	179.98(3)	175.92(3)	173.728(17)	160.501(13)
L1-Pt-Cl	90.010(16)	91.11(5)	93.136(8)	95.806(11)*
L2-Pt-Cl		92.70(5)		89.886(11)*
Cl-Pt-C1	180.0	177.0(3)	180.0	178.14(13)*
L1-Pt-C1	89.990(16)	89.4(2)	86.864(9)	84.81(11)
L2-Pt-C1		86.7(2)		88.97(11)
C111-L1-Pt	110.20(9)	119.1(2)	120.37(14)	124.26(11)
C121-L1-Pt	116.09(8)	113.8(2)	118.34(13)	102.93(12)
C131-L1-Pt	120.38(9)	115.6(2)	112.20(13)	123.56(12)
C211-L2-Pt		110.5(3)		126.47(12)
C221-L2-Pt		117.3(2)		105.41(12)
C231-L2-Pt		118.5(2)		121.56(12)
C111-L1-C121	105.19(12)	99.5(3)	99.2(2)	97.37(17)
C111-L1-C131	102.39(12)	100.4(3)	102.1(2)	101.50(17)
C121-L1-C131	100.74(12)	106.1(3)	101.8(2)	101.74(18)
C211-L2-C221		103.0(4)		100.12(18)
C211-L2-C231		103.9(4)		97.19(17)
C221-L2-C231		101.7(3)		101.99(18)
L1-Pt-C1-C2	64.92(13)	87.3(7)	82.8(3)	93.3(4)
#$(^{\theta}/_{2})_{E11}$	87.3	78.7	73.4	68.5
$(^{\theta}/_{2})_{E12}$	71.5	75.3	65.2	74.5
$(^{\theta}/_{2})_{E13}$	100.3	65.1	68.8	64.3
$\theta_{E(1)}$	173	146	138	138
$(^{\theta}/_{2})_{E21}$		81.7		69.6
$(^{\theta}/_{2})_{E22}$		74.1		87.6
$(^{\theta}/_{2})_{E23}$		61.8		59.4
$\theta_{E(2)}$		145		144

* Pt-I; #$[(^{\theta}/_{2})_{E11}]$; # Half-angles as defined in literature (Tolman 1977)
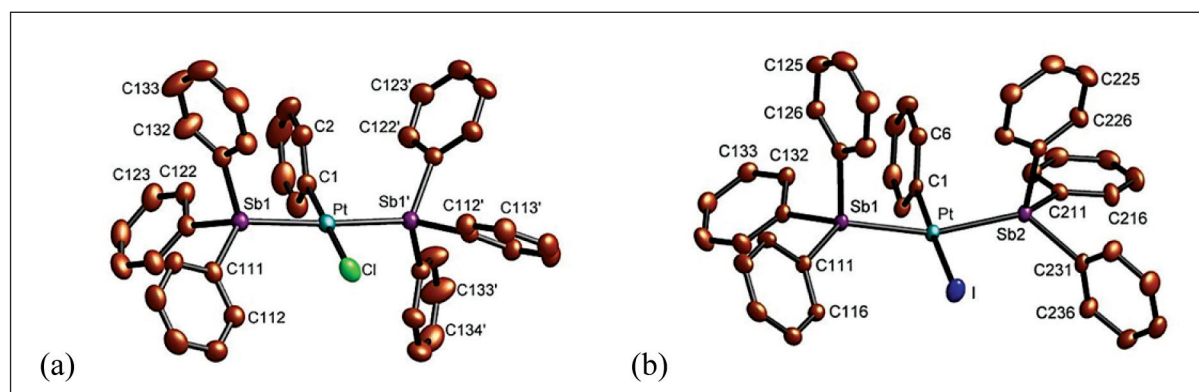
FIGURE 2: Molecular diagram showing the numbering scheme and displacement ellipsoids (30% probability) in (a) **IVa**, and (b) **IVb**. The hydrogen atoms were omitted for clarity. In the numbering scheme of the phenyl rings the first digit refers to the number of the ligand, the second to the number of the ring (1 - 3) and the third to the number of the carbon in the ring (1 - 6).

centres), but the substantial difference in size between the phenyl- and chlorido ligands significantly reduced this possibility with no disorders encountered in this study. Longer Pt-As or Pt-Sb bonds tend to result in larger distortions of the angles within the Pt coordination sphere making these systems even less prone to disorders than the corresponding phosphine complexes. The highly symmetrical geometry for complexes covered in this study does, however, result in the molecules of **IIIa** and **IVa** crystallising both on a two-fold rotation axis.

The dihedral planes described by the phenyl ligands are slightly rotated with respect to the Pt coordination plane forming angles of 64.92(13)°, 87.3(7)° and 82.8(3)° respectively for **IIa**, **IIIa** and **IVa**. The larger deviation from 90° observed in **IIa** is most likely a consequence of the significant steric crowding experienced in this tertiary ligand system.

As reported before, in the structure of **IIa** the P-C bond of 1.807(3) Å to the ferrocenyl is significantly shorter than those to the phenyl rings of 1.827(3) and 1.830(4) Å respectively (Otto and Roodt 2004). The increase in the L-C bond distances of *ca.* 1.83 to 1.93 to 2.13 Å for L = P to As to Sb is amongst other a consequence of the increase in the covalent radius of the group 15 donor atoms of 1.100, 1.210 and 1.410 Å respectively (Sheldrick 2008).

The two cyclopentadienyl rings of the ferrocenyl moiety are in an eclipsed conformation (as shown by the appropriate torsion angles close to 0°) as are normally found for a molecule substituted on one ring only. It was found that the torsion angle describing the orientation of the ferrocenyl (Pt-P-C(31)-C(41) = 43.22(15)°) has a significant effect on the cone angle of the phosphine ligand and is reported for this reason. The effective (θ_E) cone angle of the PPh_2Fc ligand was determined according to the Tolman model (Tolman 1977) as $\theta_{E(1)}$ = 168.80°. The effective (θ_E) cone angles for the $AsPh_3$ ligands were determined according to the Tolman model as $\theta_{E(1)}$ = 139.34° and $\theta_{E(2)}$ = 139.38° for As(1) and As(2) respectively which is in good

agreement with an expected angle smaller than the value of 145° for PPh_3. The effective (θ_E) cone angle for the $SbPh_3$ ligand was determined as $\theta_{E(1)}$ = 135.13° which is also in good agreement with an expected angle smaller than the value of 145° for PPh_3.

In general, the relative long Pt-Cl bond distances of 2.387(2) - 2.4574(18) Å *trans* to the phenyl- and substituted phenyl ligands, for the complexes listed in Table 3 are in agreement with the large *trans* influence exhibited by σ donor ligands coordinated *via* a carbon atom. The L-Pt-L angles show a rough correlation with the steric size of the neutral ligands: the larger the ligands the closer the angle becomes to 180°.

The Pt-C and Pt-L bond distances determined in this study are within ranges established for these types of bonds. The Pt-Cl bond distances of 2.408(5), 2.4575(18) and 2.387(2) Å for the range of complexes *trans*-[PtPh(L)$_2$Cl] (L = PPh$_3$; AsPh$_3$ and SbPh$_3$) show an unexpected large variation. An exceptionally long Pt-Cl bond of 2.4575(18) Å was obtained for **IIIa** and may be attributed to steric interactions between the chlorido and arsine ligands as the arsine ligands are distorted towards the phenyl ligand with an angle of 175.89(3)°. The short Pt-Cl bond distance of 2.387(2) Å found in **IVa** could be attributed to a combination of an electron deficient metal centre and a severely distorted Sb-Pt-Sb angle of 173.728(17)°. This distortion may be a result of the long Pt-Sb bond distances of 2.5419(5) Å allowing the ligands to be forced closer together without experiencing significant steric interactions with the chlorido ligand.

The structure of **IVb** indicates a severely distorted square planar geometry with the phenyl and iodo ligands *trans* to each other as expected after substitution of chloride from **IVa**. The Sb-Pt-Sb′ bond angle of 160.501(13)° is very unusual and may be indicative of a severely electron deficient metal centre. Stibine ligands are known to form five-coordinate complexes with d^8 metal centres to stabilise the electronic requirements of these systems (Roodt, Otto and Steyl 2003). The Pt-I bond compares well with other structures in literature (Allen 2002).

TABLE 3: Comparison of structural data for the *trans*-[PtPh(L)$_2$X] complexes.

Complex	Pt-L (Å)	Pt-C (Å)	Pt-X (Å)	L-Pt-L (°)	Ref.
trans-[PtPh(SMe$_2$)$_2$Cl]	2.294(4)	1.99(1)	2.404(3)	171.38(5)	a
trans-[PtPh(SMe$_2$)$_2$Cl]	2.293(2)	2.004(5)	2.420(1)	178.50(2)	b
trans-[Pt(mesityl)(SMe$_2$)$_2$Cl]	2.292(2)	2.028(9)	2.423(3)	178.8(2)	c
trans-[Pt(p-anisyl)(SMe$_2$)$_2$Cl]	2.287(3)	2.033(8)	2.406(3)	173.9(3)	d
trans-[PtPh(SEt$_2$)$_2$Cl]	2.29(1)	2.05(4)	2.41(1)	172(1)	e
trans-[PtPh(PPh$_3$)$_2$Cl]	2.300(6)	2.00(2)	2.408(5)	176.0(2)	f
trans-[Pt(p-OMe-Ph)(PPh$_3$)$_2$Cl]	2.312(5)	2.01(1)	2.40(4)	173.7(1)	g
trans-[Pt(o-Tol)(PEt$_3$)$_2$Cl]	2.292(6)	2.05(1)	2.412(4)	176.9(2)	h
trans-[PtPh(PPh$_2$Fc)$_2$Cl]	2.3298(8)	2.022(4)	2.3988(12)	179.98(3)	TW
trans-[PtPh(AsPh$_3$)$_2$Cl]	2.3986(8)	2.042(8)	2.4575(18)	175.92(3)	TW
trans-[PtPh(SbPh$_3$)$_2$Cl]	2.5419(5)	2.018(6)	2.387(2)	173.728(17)	TW
trans-[PtPh(SMe$_2$)$_2$Cl]	2.294(4)	1.99(1)	2.404(3)	171.38(5)	i
trans-[PtPh(SbPh$_3$)$_2$I]	2.5419(5)	2.018(6)	2.387(2)	173.728(17)	TW

a = (Kapoor, et al. 1996) b = (Kapoor, et al. 1996) c = (Wendt, Oskarsson, et al. 1997) d = (Wendt, Oskarsson, et al. 1997) e = (Wendt, Oskarsson, et al. 1997) f = (Conzelmann, et al. 1984) g = (Khanna, et al. 1995) h = (Rieger, Carpenter and Rieger 1993) i = (Wendt, Oskarsson, et al. 1997) TW = This Work

Kinetics

In an attempt to limit solvent contributions as far as possible, the complexes' kinetic behaviour was specifically investigated in non-coordinating, non-polar solvents. This resulted in poor solubility of the complexes being investigated, limiting the study to benzene, chloroform or dichloromethane. This in turn restricted potential ligands to a large extent with the only possibilities being salts containing organic cations (such as Bu_4N^+ and PPh_4^+), as well as pyridine and substituted derivatives thereof, *e.g.* 4-Br-pyridine; 4-Me-pyridine and 4-dimethyl amino pyridine were all preliminarily investigated.

As indicated earlier, note that the liquid state reactants studied kinetically are denoted by *Arabic numericals* **1 – 4**, and when referring to related literature complexes, **5 – 10**, as discussed below.

Upon evaluation of the reactions between the platinum complexes with pyridine and its derivatives it was found that substitution of the As and Sb ligands also occurred. Since the aim of the study was to investigate only chlorido substitution from the parent complexes, these types of entering nucleophiles were subsequently ruled out. The salts containing PPh_4^+ and $AsPh_4^+$ as cations exhibited large molar absorptivities in the UV region where most of the reactions were investigated and could for this reason, also not be included. Stability checks with Bu_4NI, Bu_4NSCN (slow decomposition) and Et_4NBr (hygroscopic) in the potential solvents showed the most feasible combination to be Bu_4NI in chloroform and was thus finally selected for the kinetic investigations. The crystal structure of *trans*-[PtPh(PPh₃)₂(NCS)], obtained from these preliminary investigations, has been published previously (Otto and Roodt 2005). The N-coordination observed in this complex is indicative of a sterically strained environment.

The complexes investigated in the kinetic study were unambiguously characterised using X-ray crystallography and multi nuclear NMR spectroscopy as described above. ^{1}H, ^{31}P and [195]Pt NMR, as applicable, were used to verify that only the chlorido ligand was substituted for iodide during the first and only reaction in all cases. It has been observed in the analogous *trans*-[PtMe(L)₂Cl] systems that prolonged standing (a few days) of the solutions did, however, yield the unexpected substitution products *trans*-[Pt(I)₂(L)₂] in a few cases. In this regard it was reported previously that *trans*-[Pt(I)₂(AsPh₃)₂] was isolated from a solution of *trans*-[PtMe(AsPh₃)₂Cl] and Bu_4NI in chloroform. This was identified as a potential problem when investigating extremely slow reactions, such as encountered in the cases of *trans*-[PtPh(L)₂Cl] (L = PPh₃ and PPh₂Fc). It was, however, verified in these cases that no traces of the corresponding *trans*-[Pt(I)₂(L)₂] complexes were being formed by comparing ^{31}P NMR spectra of the reaction mixtures with that of the pure *trans*-[Pt(I)₂(L)₂] (L = PPh₃ and PPh₂Fc) complexes. The additional steric demand of the phenyl, as compared to methyl, is expected to inhibit

the formation of the six coordinate Pt(IV) oxidative addition intermediate required for this conversion.

Eqn. 1 was used to fit all the kinetic results obtained during this study as shown below; the profiles of the observed pseudo first-order constants clearly fitting the complete relationship as predicted, see Figures 3 and 4. It is however clear that under equilibrium conditions (*i.e.* relative small K_{eq} values), the concentration of the leaving Cl^- can contribute significantly to the overall rate. It is thus imperative that pseudo first-order conditions in terms of $[Cl^-]$, with respect to [Pt], be employed. In this regard it was observed that the $[Cl^-]$ exhibited varied influences on the different complexes under investigation ranging from almost negligible to significant. A complete investigation in this regard was, however, not foreseen as part of this study but should be addressed in future.

Unfortunately, the equilibrium constants for the reactions could not be determined using standard spectrophotometric techniques as the ligand (Bu_4NI) also absorbs strongly in the same region where the spectral changes are taking place. For this reason, multi-nuclear NMR spectroscopy was utilised to determine the equilibrium constants where possible. ^{31}P NMR was used for the *trans*-[PtPh(L)₂Cl] (L = PPh₃ and PPh₂Fc) complexes which were determined at 40 °C. The observed rate constants for the latter complex were simultaneously determined by NMR, while the e.s.d.'s on the equilibrium constants were estimated to be 15 – 20% of the values obtained by the NMR studies.

A graphical comparison of the reactions of the *trans*-[PtPh(L)₂Cl] complexes with Bu_4NI in chloroform medium at 40 °C is presented in Figure 3 while the rate constants for the reactions are summarised in Table 4.
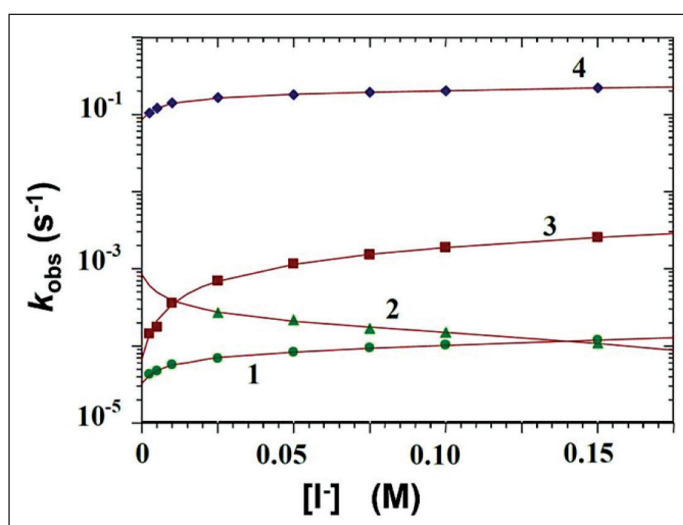
FIGURE 3: [I⁻] dependence of the observed pseudo first-order rate constants (logarithmic scale) for the *trans*-[PtPh(L)₂Cl] complexes in chloroform at 40 °C, illustrating the significant variation in reactivity and profile. Complexes are *trans*-[PtPh(L)₂Cl] (L = PPh₃, **1**; PPh₂Fc, **2**; AsPh₃, **3**; SbPh₃, **4**).

TABLE 4: Equilibrium-, first- and second-order rate constants for the reactions of the *trans*-[PtPh(L)₂Cl] complexes with Bu₄NI in chloroform at 40 °C. Complexes are *trans*-[PtPh(L)₂Cl] (L = PPh₃, **1**; PPh₂Fc, **2**; AsPh₃, **3**; SbPh₃, **4**)

Complex	K_{eq}	$10^3 k_{12}$ (M⁻¹ s⁻¹)	$10^3 k_{13}$ (s⁻¹)	$10^4 k'_{13}$ # (M⁻¹ s⁻¹)	k_{32}/k_{31}	δ(Pt) (ppm)
1	0.6 ± 0.1	0.37 ± 0.03	0.066 ± 0.003	0.053 ± 0.002	0.103 ± 0.018	−4377
2	0.1 ± 0.1	−0.67 ± 0.14*	0.20 ± 0.02	0.160 ± 0.016	0.5 ± 0.3	−4300
3	1.2 ± 0.3	11.6 ± 0.9	1.0 ± 0.2	0.80 ± 0.16	0.50 ± 0.13	−4316
4	0.6 ± 0.1	280 ± 30	181 ± 4	145 ± 0.003	0.264 ± 0.009	−4136

k'_{13}=k_{13}/[12.5 M (CHCl₃)]; * See text

The pseudo first-order rate constants of the reactions are plotted on a logarithmic scale (Figure 3) to enable further illustration of the significant difference in the reactivity of the complexes. It is clear from Table 4 and Figure 3 that the series of reactivity (most to least) for the *trans*-[PtPh(L)₂Cl] complexes are L = SbPh₃ > AsPh₃ > PPh₂Fc ≈ PPh₃. A relative range of reactivity spanning almost *four orders-of-magnitude* was observed (Figure 3). All the graphs displayed limiting kinetics, indicating that equilibria play an important role during the overall reaction, especially at lower levels of iodide. This is similar to that observed for the *trans*-[PtH(L)₂Cl] and *trans*-[PtMe(L)₂Cl] described previously (Otto, Botha and Roodt 2018).

The two phosphine-containing complexes (**1** and **2**) have comparable reactivities while the arsine (**3**) and stibine (**4**) complexes are substantially more reactive. The reactions of **1** and **2** were extremely slow and were hence investigated in the absence of added chloride. As a consequence, the rate constants were calculated by fixing the [Cl⁻] in Eq. 1 equal to that of the [Pt] (0.25 or 2.5 mmol dm⁻³) and using the values for K_{eq} determined by ³¹P NMR at 40 °C. In the case of **3** and **4** the value for the equilibrium constants were first obtained by refining it along with the other constants in the least-squares fit and fixing it afterwards to obtain more accurate values for the other constants. For **1**, **3** and **4** (L = PPh₃, AsPh₃ and SbPh₃) it was found that the k_{12} route is more rapid than the k_{13} route, but this does not hold for the severely crowded **2** (L = PPh₂Fc) where the solvent assisted pathway seems to be the route of choice. In **2** the initial inverse dependence on the [I⁻] is clear, most probably indicative of large steric effect induced by the bulky ferrocenyl substituent, suppressing the solvent pathway at increasing nucleophile concentrations. During the fitting of the kinetic data for **2** attempts were made to fix the value for k_{12} at zero, however this resulted in unsatisfactory least-squares fits being obtained and hence it was allowed to refine to a slightly negative value. Due to the fact that a significantly higher platinum concentration (2.5 mM) had to be used to conduct the NMR experiments the iodide concentration could not be lowered to describe the behaviour of the reaction at lower concentrations in more detail.

The observation that **4** is much more reactive than the other complexes can be attributed to a significantly more electrophilic metal centre (very short Pt-Cl bond distance of 2.387(2) Å) in conjunction with the fact that it is *much more accessible* due to the substantially elongated Pt-Sb bond

distances of 2.5419(5) Å as observed from the structural investigations of **IVa** and **IVb** (Figure 2). It was also shown that the average cone angle of the SbPh₃ ligand, determined as 138°, is significantly smaller than in the phosphine and arsine ligands (173° and 146° for PPh₂Fc and AsPh₃, respectively), see Table 2. Moreover, this is even better illustrated by considering the significant increase in the L1-L2 bond distances, which range from 4.660(1) to 4.794(1) to 5.080(1) Å for **IIa**, **IIIa** and **IVa**, respectively, rendering the Pt(II) metal centre in **4** clearly much more accessible than in **3**, and particularly, than in **2** and **1**.

The [I⁻] and temperature dependence of the observed pseudo first-order rate constants of **3** and **4** are shown in Figure 4.
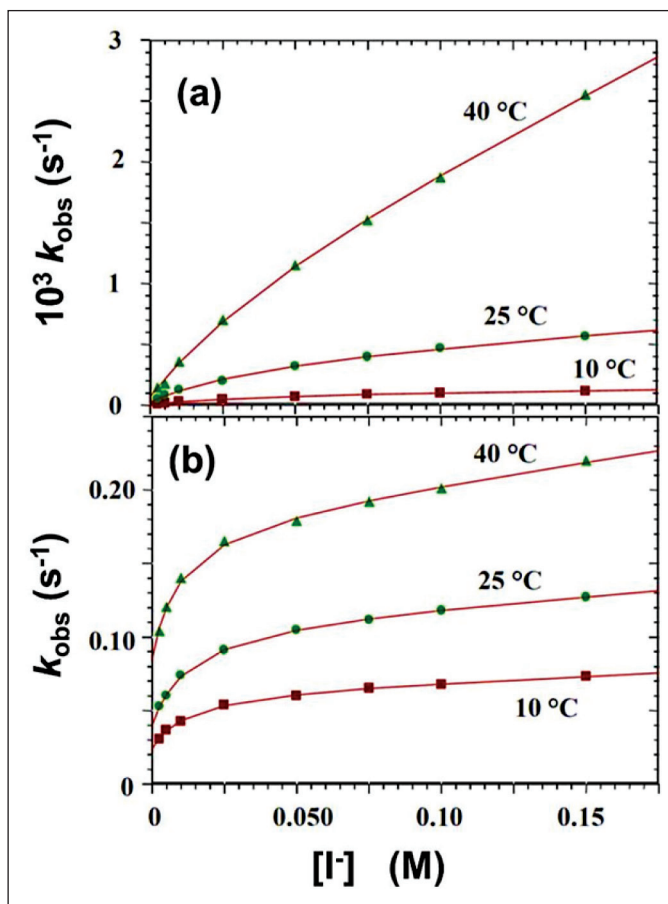
FIGURE 4: Temperature and iodide concentration dependence of the observed pseudo first-order rate constants of (a) **3** and (b) **4**.
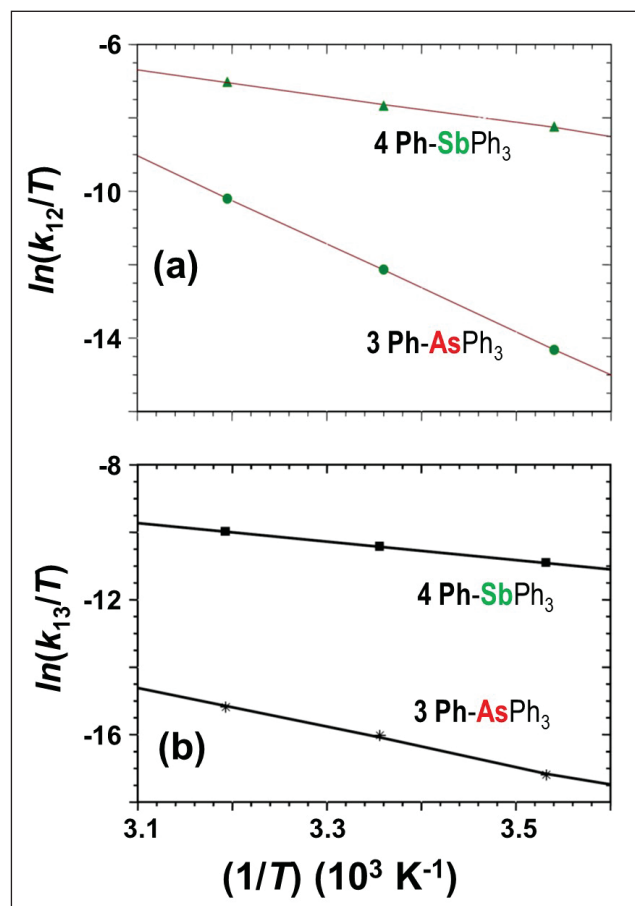
FIGURE 5: Eyring plot for the (a) k_{12} and (b) k_{13} rate constants for **3** and **4** in chloroform.

It is clear that at higher [I⁻], the graphs shown in Fig. 4 can be simplified to describe the usual two-term rate law, as given in Eq. 3. Graphical comparisons of the Eyring plots for **3** and **4** are presented in Figure 5(a) for the k_{12} and Figure 5(b) for the k'_{13} reaction routes respectively, with the resulting activation parameters listed in Table 5.

The activation parameters in general indicate that the usual associative mechanism of activation still holds in these complexes as large negative $\Delta S^{\neq}$ values were obtained for both the direct- and solvent-assisted pathways. The exception here is the $\Delta S^{\neq}$ value of 36 ± 2 J K^{-1} mol^{-1} obtained for the k_{12} route for **3**. Interestingly, however, while the entropy of activation for the k_{12} pathway is positive, a large negative value was still obtained for the solvent assisted k'_{13} route. The other $\Delta S^{\neq}$ values for k_{12} and k'_{13}, as expected for an associative mechanism of activation, range from -157 ± 4 to -207 ± 4 J K^{-1} mol^{-1}. In all cases the $\Delta S^{\neq}$ values for the k'_{13} route was found to be larger than that for the k_{12} route. If one keeps in mind that an exceptionally long Pt-Cl bond distance of 2.4575(18) Å was observed for **3** in contrast to the short 2.387(2) Å obtained for **4**, it is clear that **4** is both sterically less crowded as well as less electron rich. Both these characteristics are expected to favour an associative mode of activation (less randomness) during substitution reactions.
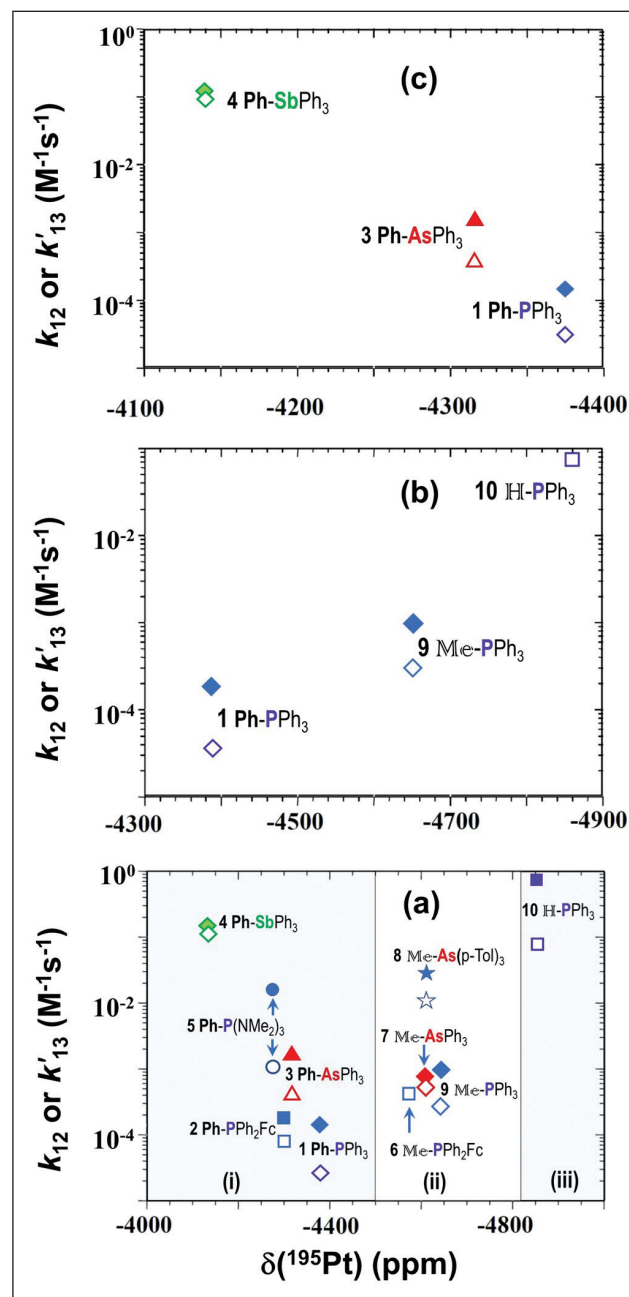
FIGURE 6: Plots of second-order rate constants (k_{12} = *filled* symbols and k'$_{13}$ = *open* symbols, where $k'_{13}=k_{13}/[12.5$ M (CHCl$_3$)]) at 25 °C vs. ^{195}Pt chemical shift, $\delta(^{195}$Pt): (a) All phenyl-, methyl- and hydrido complexes of the form *trans*-[PtR(YX$_3)_2$Cl] listed in Table 10, with Y=P, As or Sb as donor atom; X=mono-anionic alkyl or aryl substituents; R⁻ = (i) Ph, (ii) CH$_3$ and (iii) H. The donor atoms **Y** within the complexes are indicated in *green* (SbPh$_3$), *blue* (PX$_3$) and *red* (AsX$_3$), respectively; (b) PPh$_3$ complexes for R⁻ = Ph, CH$_3$, and H; (c) YPh$_3$ complexes for **Y**=P, As and Sb.

TABLE 5: Activation parameters determined by the exponential form of the Eyring equation for **3** and **4** with Bu$_4$NI in chloroform.

Complex	k_{12}		k_{13}	
	$\Delta H^{\neq}$	$\Delta S^{\neq}$	$\Delta H^{\neq}$	$\Delta S^{\neq}$
	(kJ mol^{-1})	(J K^{-1} mol^{-1})	(kJ mol^{-1})	(J K^{-1} mol^{-1})
3	99.8 ± 0.6	36 ± 2	45 ± 2	-181 ± 7
4	31 ± 1	-157 ± 4	22.91 ± 0.11	-207.3 ± 0.4

TABLE 6: Rate constants for related complexes in chloroform at 25 °C as a function of ^{195}Pt chemical shift.

No.	Range[a]	Complex	$10^3 k_{12}$ (M^{-1} s^{-1})	$10^4 k'_{13}$ (M^{-1} s^{-1})	$\delta(^{195}$Pt) (ppm)
1		trans-[PtPh(PPh$_3$)$_2$Cl] [b]	0.14 ± 0.03	0.025 ± 0.003	-4377
2	(i)	trans-[PtPh(PPh$_2$Fc)$_2$Cl] [b]	0.2	0.075 ± 0.005	-4300
3		trans-[PtPh(AsPh$_3$)$_2$Cl]	1.6 ± 0.3	0.33 ± 0.05	-4316
4		trans-[PtPh(SbPh$_3$)$_2$Cl]	143 ± 10	88.4 ± 1.1	-4136
5		trans-[PtMe{P(NMe$_2$)$_3$}$_2$Cl]	13.89 ± 0.16	0.9936 ± 0.0012	-4277
6		trans-[PtMe(PPh$_2$Fc)$_2$Cl]	0	0.317 ± 0.010	-4575
7	(ii)	trans-[PtMe(AsPh$_3$)$_2$Cl]	0.2 ± 0.4	8.3 ± 0.8	-4608
8		trans-[PtMe{As(p-Tol)$_3$}$_2$Cl]	2.79 ± 0.04	0.42 ± 0.03	-4611
9		trans-[PtMe(PPh$_3$)$_2$Cl]	0.091 ± 0.010	0.203 ± 0.010	-4646
10	(iii)	trans-[PtH(PPh$_3$)$_2$Cl]	0	62.2 ± 0.4	-4858

[a] Illustrated in Fig. 6(a); [b] Values estimated from data obtained at 40 °C assuming the rates approximately halve with ca. every 10 °C decrease in temperature

Table 6 lists both the direct- (k_{12}) and solvent route rate constants ($k_{13'}$) as a function of ^{195}Pt chemical shifts. The chemical shift of a specific nucleus gives an indication of the electronic environment; thus, one might suspect a rough correlation to exist between the reactivity of a complex and the chemical shift of the metal centre. In Figure 6 the first- and second-order rate constants of the individual complexes, or more correctly a range of *closely analogous* ones, are plotted against their ^{195}Pt chemical shifts.

In general, no clear correlation was observed between δ(Pt) and the reactivity of the *trans*-[PtR(YX$_3$)$_2$Cl] complexes as is illustrated in Figure 6a. However, the phenyl complexes (see (i)) clearly are grouped between -4000 to -4500 ppm, the methyl complexes from -4500 to ca. -4800 ppm (see (ii)), and the hydrido complex at -4810 ppm (iii). Although the data is certainly not convincing and definitely require a larger statistical sample range, the tendency is certainly worth noting.

However, if the complex ranges are examined individually, a tendency of a correlation within *closely analogous* complexes does exist. In Figure 6b the reactivity *vs.* δ(Pt) values for the *trans*-[PtPh(YPh$_3$)$_2$Cl] (Y = P; As and Sb) complexes display a definite trend with a decrease in reactivity corresponding to a shift toward higher field, generally associated with increased electronic shielding. This is in accordance with the understanding that an associative mechanism of activation would be favoured as the metal centre becomes more electrophilic. Another interesting observation is the increase in the difference between k_{12} and $k_{13'}$ with an increase in electronic shielding of the platinum centre indicating a larger extent of discrimination between different entering nucleophiles as the metal centre becomes less electrophilic.

Similarly, in Figure 6c the complexes of the general form, *trans*-[PtR(PPh$_3$)$_2$Cl] (R$^-$ = CH$_3$$^-$, H$^-$ and Ph$^-$) is shown. Only the $k_{13'}$ value for the hydride complex is reported since the value for the k_{12} value was fixed at 0. The most important observation made from this figure is that an increase in the rate constants corresponds to an increase in electronic shielding of the platinum centre. This is contrary to what would be expected from an electronic perspective with the observed trend predominantly attributed to a decrease in the steric crowding of the metal centre going from Ph > Me > H.

Summary and Conclusions

A good correlation was found when comparing the results obtained from this kinetic study with some relevant examples taken from the literature. Most of the previously reported studies were conducted in methanol (a coordinating solvent) on complexes containing substantially smaller *cis* ligands; especially PEt$_3$ was quite extensively used. In complexes of the form *trans*-[PtR(L)$_2$X] (R = hydrido, alkyl and aryl; L = PEt$_3$, SMe$_2$ and SEt$_2$) a decrease in reactivity was observed with increased steric size of the substituted phenyl ligands as R ligands (Cusumano, et al. 1979) (Ricevuto, Romeo and Trozzi 1974) (Faraone, et al. 1974). The reactivity showed a significant decrease in the order hydride > alkyl > aryl, but in all cases the normal associative mechanism was still active.

A study (Wendt and Elding 1997) on complexes of the form [Pt(I)$_3$L]$^-$ (L = PPh$_3$ and SbPh$_3$) indicated that the stibine ligand exhibits a more significant *trans* effect than the phosphine analog. The X-ray crystal structures of the two complexes, however, suggested that the stibine ligand has a smaller *trans* influence, and hence the increase in reactivity must arise from stabilisation of the transition state, i.e., the *trans* effect. These results seem to indicate that the SbPh$_3$ ligand is a better π acceptor than PPh$_3$ which is, in conjunction with a decrease in steric crowding, also the conclusion that can be drawn from the current investigation.

The general perception amongst chemists is that the substitution behaviour of square-planar complexes is clear and simple with everything well understood. It is covered extensively in many textbooks illustrating various principles like the *cis*- and *trans* effects. With this study we investigated the reactivity of a range of iso-electronic complexes and have shown that reasonable correlations between the kinetic- and structural data exist. It is furthermore clear that care needs to be taken when interpretations are done, as these systems could be *significantly* more complex than anticipated. Thus, the importance of a thorough understanding of the basic

principles of reaction kinetics and the examining of the *complete* reaction mechanism for these reactions were clearly illustrated.

As indicated earlier, substitution reactions are very important in many fundamental and applied processes such as catalytic processes, metal extraction, medicinal inorganic chemistry and environmental reactions, typically associated with carbon dioxide fixation. Thus, detailed mechanistic and time resolved information as provided herein is important when considering similar systems for appropriate application.

Acknowledgments

Author Contributions

SO did practical work and wrote the first draft of paper. OTA assisted with crystallography and additional modification, while AR was supervisor of the study and wrote the final manuscript.

References

Alibrandi, G., L. M. Scolaro, and R. Romeo. 1991. "A new reaction pathway for the Geometrical Isomerization of Monoalkyl Complexes of Platinum(II) and Kinetic Behavior of cis-[Pt(PEt$_3$)$_2$(neopentyl)Cl]." *Inorganic Chemistry* 30: 4007-4013.

Alibrandi, G., M. Cusumano, D. Minniti, L. M. Scolaro, and R. Romeo. 1989. "Competitive uncatalyzed geometrical isomerization and. beta.-hydride elimination of alkyl complexes of platinum(II)." *Inorg. Chem.* 28: 342-347.

Allen, F. H. 2002. "The Cambridge Structural Database: a quarter of a million crystal structures and rising." *Cambridge Structural Database, Version XX, XX 2011/12 update.* B58: 380-388.

Baddley, W. H., and F. Basolo. 1966. "Preparation and Kinetic Study of Some Sterically Hindered Palladium (II) Complexes." *J. Am. Chem. Soc.* 88: 2944-2950.

Berger, J., M. Kotowski, R. van Eldik, U. Frey, L. Helm, and A. E. Merbach. 1989. "Kinetics and mechanism of solvent-exchange and anation reactions of sterically hindered diethylenetriamine complexes of palladium (II) in aqueous solution." *Inorg. Chem.* 28: 3759-3765.

Brandenburg, K. 1998. "DIAMOND Version 2.1." Bonn, Germany.: Crystal Impact.

Bruker-AXS-Inc. 2007. "Bruker SAINT-Plus and SADABS." Madison, Wisconsin, USA.

Bugarčić, Ž. D., J. Bogojeski, B. Petrović, Z. D. S. Hochreuther, and R. van Eldik. 2012. "Mechanistic studies on the reactions of platinum (II) complexes with nitrogen-and sulfur-donor biomolecules." *Dalton Trans.* 41: 12329-12345.

Chatt, J., and B. L. Shaw. 1959. "Alkyls and aryls of transition metals; Part I; Complex methylplatinum(II) derivatives." *J. Chem. Soc.* 705-716.

Chatt, J., L. M. Vallarino, and L. M. Venanzi. 1957. "Olefin Coordination Compounds. Part IV. Diene Complexes of Platinum(II). The Structure of Hofmann and van Narbutt's [Dicyclopentadiene(RO)PtCL]." *J. Chem. Soc.* 2496-2505.

Conzelmann, W., J. D. Koola, U. Kunze, and J. Strähle. 1984. "Molecular structure of trans-chloro(η1-phenyl)-bis(triphenylphosphine)platinum(II)." *Inorg. Chim. Acta* 89: 147-149.

Crespo, M., M. Martínez, S. M. Nabavizadeh, and M. Rashidi. 2014. "Kinetico-mechanistic studies on CX (X = H, F, Cl, Br, I) bond activation reactions on organoplatinum(II) complexes." *Coord. Chem. Rev.* 279: 115-140.

Cusumano, M., R. Marricchi, R. Romeo, V. Ricevuto, and U. Belluco. 1979. "Displacement of chloride under the trans-effect of strong σ-donor groups in Pt (II) complexes." *Inorg. Chim. Acta* 34: 169-174.

De Waal, D.J.A., and W. Robb. 1978. "Experimental evidence for a more complete rate law for nucleophilic substitution at square planar metal complex centers. Kinetics and mechanism of ligand replacement in the complex cycloocta-1,5-dienetricyclohexylphosphinechlororhodium(I)." *Inorg. Chim. Acta* 26: 91-96.

Dobrynin, M. V., Pretorius, C., Kama, D.V., Roodt, A., Boyarskiy, V.P., and Islamova, R. M. 2019. Rhodium(I)-catalysed cross-linking of polysiloxanes conducted at room temperature. *Journal of Catalysis* 372: 193-200.

Elding, L. I., B. Kellenberger, and L .M. Venanzi. 1983. "Transition Metal Complexes with Bidentate Ligands Spanning trans-Positions. XII†. Steric effects in the kinetics and mechanism of substitutions at hydride and methyl bisphosphine platinum (II) complexes." *Helv. Chim. Acta* 66: 1676-1690.

Elding, L.I., and A.-B. Gröning. 1980. "Solvent paths for square-planar substitutions. Part 2. Reactions between aqua chloroplatinates (II) and ethane. ." *Inorg. Chim. Acta* 38: 59-66.

Faraone, G., V. Ricevuto, R. Romeo, and M. Trozzi. 1974. "Steric effects in substitution reactions of cis- and trans-arylchlorobis-(triethylphosphine) platinum(II) complexes: new kinetic data for the approach to the problem of transition-state geometry." *J. Chem. Soc. Dalton Trans.* 1377-1380.

Frey, U., L. Helm, A. E. Merbach, and R. Romeo. 1989. "Dissociative Substitution in Four-Coordinate Planar Platinum(II) Complexes As Evidenced by Variable-Pressure High-Resolution Proton NMR Magnetization Transfer Experiments." *J. Am. Chem. Soc.* 111: 8161-8165.

Goddard, J. B., and F. Basolo. 1968. "Rates and mechanism of substitution reactions of sterically hindered palladium (II) complexes." *Inorg. Chem.* 7: 936-943.

Hennion, C., K. Johanson, O. F. Wendt, and A. Roodt. 2013. "Kinetic and mechanistic investigation of the substitution reactions of four and five co-ordinated rhodium stibine complexes with a bulky phosphite. ." *Dalton Trans.* 42: 14134-14139.

Hoffmann, K., I. Łakomska, J. Wiśniewska, A. Kaczmarek-Kędziera, and J. Wietrzyk. 2015. "Acetate platinum(II) compound with 5,7-ditertbutyl-1,2,4-triazolo[1,5-a]pyrimidine that overcomes cisplatin resistance: structural characterization, in vitro cytotoxicity, and kinetic studies." *J. Coord. Chem.* 68: 3193-3208.

Johnstone, T. C., K. Suntharalingam, and S. J. Lippard. 2016. "The Next Generation of Platinum Drugs: Targeted Pt(II) Agents, Nanoparticle Delivery, and Pt(IV) Prodrugs." *Chem. Rev.* 116: 3436-3486.

Kapoor, P., V. Y. Kukushkin, K. Lövqvist, and Å. Oskarsson. 1996. "Trans influence in platinum(II) complexes. Phenylation of Pt(II) dialkylsulfide complexes by BPh4– and SnPh3H. Crystal structures of two polymorphs of trans-chlorobis(dimethylsulfide)(phenyl)platinum(II)." *J. Organomet. Chem.* 1-2: 71-70.

Khanna, A., B. L. Khandelwal, A. K. Saxena, and T. P. Singh. 1995. "Dichloromethane assisted oxidation of Pt(O) via cleavage of Te=C bond of an asymmetric telluride leading to the formation of trans-[PtCl(Ar)(PPh$_3$)$_2$]." *Polyhedron* 14: 2705-2710.

Kubota, M., R. K. Rothrock, M. R. Kernan, and B. R. Haven. 1982. "Rearrangement of alkyl- and arylsulfinato-S to alkyl- and arylsulfinato-O,O' complexes of platinum(II). Barrier to desulfonylation." *Inorg. Chem.* 21: 2491-2493.

Kukushkin, V. Y., K. Lövqvist, B. Norén, Å. Oskarsson, and L. I. Elding. 1992. "Phenylation of Platinum(II) thioether complexes by tetraphenylborate(III) in solid state and nitromethane solution." *Phosphorous, Sulfur and Silicon* 73: 253-255.

Maidich, L., Zucca, A., Clarkson, G. J., and Rourke, J. P. 2013. "Oxidative Addition of MeI to a Rollover Complex of Platinum(II): Isolation of the Kinetic Product." *Organometallics* 32: 3371-3375.

MicroMath. 1990. «Scientist for Windows, Least-squares Parameter Estimation, Version 4.00.950.»

Minnitti, D., G. Alibrandi, M. L. Tobe, and R. Romeo. 1987. «Dissociative Substitution in Four-Coordinate Planar Platinum(II) Complexes. 3. Kinetics of the Displacement of Sulfur Donors from cis-Dimethylbis(dimethyl sulfoxide)- and cis-Dimethylbis(dimethyl sulfide)platinum(II) by Bidentate Ligands.» *Inorg. Chem.* 26: 3956-3960.

OLIS. n.d. "On-Line Instrument-Systems Inc." Jefferson, Ga 30549.

Otto, S., A. Roodt, and J. G. Leipoldt. 1995. "Structural trans effect in trans-[PtMeX(PPh$_3$)$_2$] complexes: a comparative ^{1}H NMR study and the crystal structure of trans-[PtMeCl(PPh$_3$)$_2$]." *S.A. J. Chem.* 48 (3-4): 114-116.

Otto, S., and A. Roodt. 2002b. "Equilibrium, solid state behavior and reactions of four and five co-ordinate carbonyl stibine complexes of rhodium. Crystal Structures of trans-[Rh(Cl)(CO)(SbPh$_3$)$_2$], trans-[Rh(Cl)(CO)(SbPh$_3$)$_3$] and trans-[Rh(I)$_2$(CH$_3$)(CO)(SbPh$_3$)$_2$]." *Inorg. Chim. Acta* 331: 199-207.

Otto, S., and A. Roodt. 2004. "Quantifying the electronic cis effect of phosphine, arsine and stibine ligands by use of rhodium(I) Vaska-type complexes." *Inorg. Chim. Acta* 357: 1-10.

Otto, S., and A. Roodt. 2006. "Reactivity studies of trans-[PtClMe(SMe$_2$)$_2$] towards anionic and neutral ligand substitution processes." *J. Organomet. Chem.* 691: 4626-4632.

Otto, S., and A. Roodt. 2008. "Solvent induced oxidative addition and phenyl migration in trans-[RhCl(CO)(SbPh$_3$)$_3$]: Crystal structure of trans-mer-[Rh(Cl)$_2$(Ph)(SbPh$_3$)$_3$]." *Inorg. Chem. Commun.* 11: 114-116.

Otto, S., and A. Roodt. 2005. "Structure of trans-(Isothiocyanato-jN)phenylbis (triphenylphosphine-P)platinum(II)." *Acta Cryst.* E61: m1545-1547.

Otto, S., and A. Roodt. 2002a. "trans-Carbonyliodotris(triphenylstibine-[kappa]Sb) rhodium(I)." *Acta Cryst.* C58: m565-m566.

Otto, S., E Botha, and A. Roodt. 2018. "Structure and Reactivity Relationships in Methyl and Hydrido Complexes of Platinum (II) by Group 15 Donor Atom Ligands." *Croatica Chemica Acta* 91: 265–279.

Palmer, D. A., R. Schmidt, R. van Eldik, and H. Kelm. 1978. "Temperature and pressure dependencies of the anation of Pd(Me)(Et$_4$dien)OH$_2^+$ by chloride ion in acidic aqueous solution. A mixing system for studying the kinetics of moderately fast reactions under pressure." *Inorg. Chim. Acta* 29: 261-265.

Palmer, D.A., and H. Kelm. 1975. "Evidence for a dual mechanisms in reactions of [Pd(Et$_4$dien) X]$^+$ complexes." *Inorg. Chim. Acta* 14: L27-L29.

Pienaar, J. J., M. Kotowski, and R. van Eldik. 1989. "Volume Profiles for Solvolysis Reactions of Sterically Hindered Diethylenetriamine Complexes of Palladium (II) in Aqueous Solution." *Inorg. Chem.* 28: 373-375.

Plutino, M. R., S. Otto, A. Roodt, and L. I. Elding. 1999. "Reaction Mechanism for Olefin Exchange at Chloro Ethene Complexes of Platinum(II)." *Inorg. Chem.* 38: 1233-1238.

Pope, W. J., and S. J. Peachey. 1907. "A new class of organo-metallic compounds. Preliminary notice. Trimethyl Platini Methyl hydroxide and its salts." *Proc. Chem. Soc.* 23: 86-87.

Ricevuto, V., R. Romeo, and M. Trozzi. 1974. "Kinetics and mechanism of replacement of chloride ion in trans-chloro-(o-tolyl)bis(triethylphosphine) platinum(II) by substituted pyridine compounds: influence of the basicity and steric hindrance of the pyridines on their reactivity." *J. Chem. Soc. Dalton Trans., 1974, 927-929.* 927-929.

Rieger, A. L., G. B. Carpenter, and P. H. Rieger. 1993. "Platinum-195 NMR and structural studies of platinum(II) o-tolyl and mesityl complexes. ." *Organometallics* 12: 842-847.

Romeo, (R., G. Alibrandi, and L. M. Scolaro. 1993. "Kinetic study of beta-hydride elimination from monoalkyl solvento complexes of platinum(II)." *Inorg. Chem.* 32: 4688-4694.

Romeo, R., A. Grassi, and L. M. Scolaro. 1992. "Factors Affecting Reaction Pathways in Nucleophilic Substitution Reactions on Platinum(II) Complexes: A Comparative Kinetic and Theoretical Study." *Inorg, Chem.* 4383-4390.

Roodt, A., H. G. Visser, and A. Brink. 2011. "Structure/reactivity relationships and mechanism from X-ray data and spectroscopic kinetic analysis." *Crystallography Reviews* 17: 241-280.

Roodt, A., S. Otto, and G. Steyl. 2003. "Structure & solution behaviour of rhodium(I) Vaska-type complexes for correlation of steric & electronic properties of tertiary phosphine ligands. ." *Coordination Chemistry Reviews* 245: 125-142.

Roulet, R., and H. B. Gray. 1972. "Mechanisms of substitution reactions of axially blocked palladium (II) complexes in different solvents ." *Inorg. Chem.* 11: 2101-2104.

Scott, J. D., and R. J. Puddephatt. 1983. "Ligand dissociation as a preliminary step in methyl-for-halogen exchange reactions of platinum(II) complexes." *Organometallics* 2: 1643-1648.

Seguin, J.-Y., and M. Zador. 1976. "Kinetics of interaction of [Pd(dien)Br]$^+$ with inosine." *Inorg. Chim. Acta* 20: 203-206.

Sheldrick, G.M. 2008. "SHELX: Programme for solving crystal structures." *Acta Cryst.* A64: 112-125.

Sollot, G. P., H. E. Mertway, S. Portnoy, and J. L. Snead. 1963. "Unsymmetrical Tertiary Phosphines of Ferrocene by Friedel-Crafts Reactions. I. Ferrocenylphenylphosphines. ." *J. Org. Chem.* 28: 1090-1092.

Tolman, C. A. 1977. "Steric effects of phosphorus ligands in organometallic chemistry and homogeneous catalysis." *Chemistry Reviews* 77: 313-348.

Van Eldik, R., D. A. Palmer, R. Schmidt, and H. Kelm. 1981. "Volumes of activation for the anation of Pd(II) substituted dien complexes by chloride ion in aqueous solution. A high pressure stopped-flow instrument for studying the kinetics of fast reactions under pressure." *Inorg. Chim. Acta* 50: 131-135.

Warsink, S., Kotze, P.D.R., Janse van Rensburg, J.M., Venter, J. A., Otto, S., Botha, E., and Roodt, A. 2018. "Kinetic-Mechanistic and Solid-State Study of the Oxidative Addition and Migratory Insertion of Iodomethane to [Rhodium(S,O-BdiPT or N,O-ox)(CO)(PR^{1}R^{2}R^3)] Complexes." *Eur. J. Inorg. Chem.* 32: 3615-3625.

Wendt, O. F., Å. Oskarsson, J. G. Leipoldt, and L.I. Elding. 1997. "Synthesis, Structure, and Reactivity of Arylchlorobis(dialkyl sulfide)platinum(II) Complexes." *Inorg. Chem.* 36: 4514-4519.

Wendt, O. F., and L. I. Elding. 1997. "trans Effect and trans influence of triphenyl-stibine and -phosphine in platinum(II) complexes. A comparative mechanistic and structural study ." *J. Chem. Soc. Dalton Trans.* 4725-4732.

Electronic Supplementary Information to:

Structure and reactivity relationships in *trans*-[PtPh(L)$_2$Cl] as observed from Cl⁻ anation by I⁻ upon interchanging phosphine, arsine and stibine (L) ligands

BOTH (A) KINETIC AND (B) CRYSTALLOGRAPHIC DATA ARE PRESENTED

A. Kinetic data (6 Tables)

The reactions of 4 different complexes with BuN$_4$I in chloroform were investigated in order to study the relative reactivity with respect to one another. Complexes **1** and **2** were only investigated at 40 °C due to their low reactivity while complexes **3** and **4** were investigated at 10, 25 and 40°C in order to obtain activation parameters for these systems.

The data for each complex is presented individually with all concentrations given in mmol dm^{-3} and all observed rate constants in s^{-1}. In all cases the reactions were carried out in dried and distilled chloroform with a final metal concentration of 0.25 mM, except in the case of *trans*-[PtPh(PPh$_2$Fc)$_2$Cl] where a final metal concentration of 2.5 mM was used to enable monitoring the reaction the reactions using ^{31}P NMR. All reactions contained additional added chloride amounting to a final concentration of 2.5 mM, except those for *trans*-[PtPh(PPh$_3$)$_2$Cl] and *trans*-[PtPh(PPh$_2$Fc)$_2$Cl] which contained no additional chloride. The final iodide concentrations were varied in the range 2.5 – 150 mM with at least a 10-fold excess of iodide to metal to ensure pseudo-first order reaction conditions.

TABLE S1: Observed pseudo first-order rate constants for *trans*-[PtPh(L)$_2$Cl] and Bu$_4$NI in chloroform at 40 °C.

[I⁻] (mM)	PPh$_3$ 10^4k_{obs} (s^{-1})	PPh$_2$Fc 10^4k_{obs} (s^{-1})	AsPh$_3$ 10^4k_{obs} (s^{-1})	SbPh$_3$ 10^4k_{obs} (s^{-1})
2.5	0.429(8)		0.514(2)	528(3)
5	0.476(5)		0.821(2)	602(3)
10	0.567(5)		1.258(4)	739(3)
25	0.690(2)	2.7(4)	2.018(12)	911(5)
52	0.831(4)	2.2(4)	3.21(4)	1047(6)
75	0.942(4)	1.7(3)	3.97(5)	1118(5)
100	1.03(7)	1.5(3)	4.68(8)	1183(6)
150	1.18(15)	1.1(2)	5.66(9)	1271(8)

TABLE S2: Equilibrium-, first- and second order rate constants for *trans*-[PtPh(L)Cl$_2$] and Bu$_4$NI in chloroform at 40 °C.

	PPh$_3$	PPh$_2$Fc	AsPh$_3$	SbPh$_3$
K_{eq} (M^{-1})	0.6(1)	0.1(1)	1.2(3)	0.6(1)
10^3k_{12} (M^{-1} s^{-1})	0.37(3)	-0.67(14)	11.6(9)	280(30)
10^3k_{13} (s^{-1})	0.066(3)	0.20(2)	1.0(2)	181(4)
10^4k_{13}' (M^{-1} s^{-1})	0.053(2)	0.160(16)	0.80(16)	145(3)
k_{32}/k_{31}	0.103(18)	0.5(3)	0.50(13)	0.264(9)

TABLE S3: Observed pseudo first-order rate constants for *trans*-[PtPh(AsPh$_3$)$_2$Cl], **3**, and *trans*-[PtClPh(SbPh$_3$)$_2$C1], **4**, with Bu$_4$NI in chloroform at 10, 25 and 40 °C.

[I⁻] (mM)	*trans*-[PtPh(AsPh$_3$)$_2$Cl] 10^4k_{obs} (s^{-1})			*trans*-[PtPh(SbPh$_3$)$_2$Cl] 10^2k_{obs} (s^{-1})		
	8.9 °C	25.0 °C	40.0 °C	10.0 °C	25.0 °C	40.0 °C
2.5	0.12(3)	0.514(2)	1.426(9)	3.06(2)	5.28(3)	10.41(8)
5	0.1747(10)	0.821(2)	1.757(9)	3.69(3)	6.02(3)	12.04(9)
10	0.2702(15)	1.258(4)	3.577(13)	4.27(3)	7.39(3)	14.01(11)
25	0.4597(9)	2.018(12)	6.98(4)	5.40(4)	9.11(5)	16.5(12)
52	0.7102(12)	3.21(4)	11.51(10)	6.02(5)	10.47(6)	17.90(14)
75	0.879(3)	3.97(5)	15.20(14)	6.51(6)	11.18(5)	19.21(17)
100	0.995(3)	4.68(8)	18.7(2)	6.77(6)	11.83(6)	20.1(2)
150	1.171(12)	5.66(9)	25.5(3)	7.32(7)	12.71(8)	22.0(2)

TABLE S4: Equilibrium-, first- and second order rate constants for *trans*-[PtPh(AsPh$_3$)$_2$Cl], **3**, and *trans*-[PtClPh(SbPh$_3$)$_2$Cl], **4**, with Bu$_4$NI in chloroform at 10, 25 and 40 °C.

	trans-[PtPh(AsPh$_3$)$_2$Cl]			*trans*-[PtPh(SbPh$_3$)$_2$Cl]		
	8.9 °C	25.0 °C	40.0 °C	10.0 °C	25.0 °C	40.0 °C
K_{eq} (M^{-1})	1.2(3)	1.2(3)	1.2(3)	0.6(1)	0.6(1)	0.6(1)
$10^3 k_{12}$ (M^{-1} s^{-1})	0.17(5)	1.6(3)	11.6(9)	75(9)	143(10)	280(30)
$10^3 k_{13}$ (s^{-1})	0.121(13)	0.41(6)	1.0(2)	64.6(12)	110.5(14)	181(4)
$10^4 k_{13}'$ (M^{-1} s^{-1})	0.097(10)	0.33(5)	0.80(16)	51.7(10)	88.4(11)	145(3)
k_{32}/k_{31}	0.049(6)	0.063(12)	0.50(13)	0.207(6)	0.199(4)	0.264(9)

TABLE S5: Activation parameters determined by the exponential form of the Eyring equation for *trans*-[PtPh(AsPh$_3$)$_2$Cl], **3**, and *trans*-[PtPh(SbPh$_3$)$_2$Cl], **4**, with Bu$_4$NI in chloroform.

Complex	k_{12}		k_{13}	
	ΔH‡ (kJ mol^{-1})	**ΔS‡** (J K^{-1} mol^{-1})	**ΔH‡** (kJ mol^{-1})	**ΔS‡** (J K^{-1} mol^{-1})
trans-[PtPh(AsPh$_3$)$_2$Cl]	99.8(6)	36(2)	45(2)	-181(7)
trans-[PtPh(SbPh$_3$)$_2$Cl]	31(1)	-157(4)	22.91(11)	-207.3(4)

TABLE S6: Activation parameters determined by the linear form of the Eyring equation for *trans*-[PtPh(AsPh$_3$)$_2$Cl], **3**, and *trans*-[PtPh(SbPh$_3$)$_2$Cl], **4**, with Bu$_4$NI in chloroform.

Complex	k_{12}		k_{13}	
	ΔH‡ (kJ mol^{-1})	**ΔS‡** (J K^{-1} mol^{-1})	**ΔH‡** (kJ mol^{-1})	**ΔS‡** (J K^{-1} mol^{-1})
trans-[PtPh(AsPh$_3$)$_2$Cl]	95.9(3)	26.6(1)	48(32)	-172(9)
trans-[PtPh(SbPh$_3$)$_2$Cl]	30(1)	-160(30)	22.6(6)	-208(204)